

PERIODIC STANDING WAVES IN THE FOCUSING NONLINEAR SCHRÖDINGER EQUATION: ROGUE WAVES AND MODULATION INSTABILITY

JINBING CHEN, DMITRY E. PELINOVSKY, AND ROBERT E. WHITE

ABSTRACT. We present exact solutions for rogue waves arising on the background of periodic standing waves in the focusing nonlinear Schrödinger equation. The exact solutions are obtained by characterizing the Lax spectrum related to the periodic standing waves and by using the one-fold Darboux transformation. The magnification factor of the rogue waves is computed in the closed analytical form. We relate the rogue wave solutions to the modulation instability of the background of the periodic standing waves.

1. INTRODUCTION

We address rogue waves described by the focusing nonlinear Schrödinger (NLS) equation:

$$(1.1) \quad i\psi_t + \frac{1}{2}\psi_{xx} + |\psi|^2\psi = 0.$$

The *canonical rogue wave* was derived in [3, 29] in the exact form:

$$(1.2) \quad \psi(x, t) = \left[1 - \frac{4(1 + 2it)}{1 + 4x^2 + 4t^2} \right] e^{it}.$$

As $|t| + |x| \rightarrow \infty$, the rogue wave (1.2) approaches the constant-amplitude wave $\psi_0(t) = e^{it}$, which is modulationally unstable [30]. The rogue wave reaches its maximum amplitude $|\psi(0, 0)| = 3$ at $(x, t) = (0, 0)$ on the background $|\psi_0(t)| = 1$, hence it achieves a triple magnification over the constant-amplitude wave. Other rational solutions for rogue waves in the NLS equation were constructed by using Darboux transformations in [4, 20, 27]. Further connection between rogue waves and the modulationally unstable constant-amplitude waves was investigated by using the inverse scattering method [7, 8, 9], asymptotic analysis [10], and the finite-gap theory [22, 23].

Periodic standing waves in the focusing NLS equation take the form

$$(1.3) \quad \psi(x, t) = U(x)e^{2ibt},$$

where U is a L -periodic complex-valued function and $2b$ is a real frequency parameter. These periodic standing waves are known to be modulationally unstable with respect to long-wave perturbations [11, 17] (see also recent studies in [18, 19]). Rogue waves have been observed numerically on the background of the modulationally unstable periodic standing waves [1, 2]. Construction of solutions of the NLS equation (1.1) for such rogue waves on the background of the periodic standing waves was first performed numerically in [12, 26] by applying the one-fold Darboux transformation to the numerically constructed solutions of the Lax equations. It was only recently in [14, 15] that the exact solutions for such rogue waves were constructed in the closed form for the dn-periodic and cn-periodic elliptic waves. A more complete analysis of rogue waves on the background of periodic elliptic waves was developed in [21].

Rogue waves on the multi-phase solutions and their magnification factors were studied in [5, 6] by using Riemann Theta functions. In the recent study [16], we have also studied numerically the rogue waves arising on the double-periodic (both in space and in time) solutions to the focusing NLS equation (1.1).

Let us now give a mathematical definition of a rogue wave on the background of a periodic standing wave. Let $\psi_0(x, t)$ be a periodic standing wave of the focusing NLS equation (1.1) in the form (1.3). We say that $\psi(x, t)$ is a *rogue wave on the background of the periodic standing wave* if it satisfies

$$(1.4) \quad \inf_{x_0, t_0, \alpha_0 \in \mathbb{R}} \sup_{x \in \mathbb{R}} |\psi(x, t) - \psi_0(x - x_0, t - t_0)e^{i\alpha_0}| \rightarrow 0 \quad \text{as } t \rightarrow \pm\infty.$$

The magnification factor of the rogue wave can be defined as a ratio of the maximum of $|\psi|$ to the maximum of $|\psi_0|$ by

$$(1.5) \quad M := \frac{\max_{(x,t) \in \mathbb{R}^2} |\psi(x, t)|}{\max_{(x,t) \in \mathbb{R}^2} |\psi_0(x, t)|}.$$

Although the physical definition of the magnification factor is the ratio of the maximum of $|\psi|$ to the mean value of $|\psi_0|$ [5, 16], which is bigger than M in (1.5), we shall use the definition (1.5) for computations of the magnification factor M in the closed analytical form.

The purpose of this work is to construct the exact solutions for rogue waves on the background of the periodic standing waves. We improve the previous work [15] in several ways.

First, we develop a general scheme for integrability of the Hamiltonian system which arises in the algebraic method with one eigenvalue [31, 32] (nonlinearization of the linear equations was pioneered in [13]). This scheme allows us to integrate the standing wave reduction of the focusing NLS equation (1.1) and to relate parameters of the periodic standing waves to eigenvalues in the Lax spectrum. This characterization of eigenvalues at the end points of the Lax spectrum complements the resolvent method developed for the same purpose in [24] (see also review in [25]).

Second, we introduce a new representation for the second growing solution to the linear equations that is applicable to every admissible eigenvalue of the Lax spectrum. The previous representation of the second growing solution in [15] only works for one eigenvalue in the Lax spectrum of the dn-periodic wave but is singular for the other eigenvalue. The new representation also gives a simpler expression to control the linear growth of the second growing solution everywhere on the (x, t) plane.

Third, we compute the explicit expression of the magnification factor M in (1.5) for a general elliptic wave solution with nontrivial phase. This analytical expression generalizes the previous computations of the magnification factors of the constant-amplitude wave, the dn-periodic wave, and the cn-periodic wave.

Fourth, we relate the existence of such rogue wave solutions to the modulation instability of the periodic wave background studied in [17]. We obtain an exceptional curve on the two-parameter plane of the general elliptic wave solutions, at which our new solution associated with one eigenvalue in the Lax spectrum is not fully localized on the (x, t) plane and violates the definition (1.4) of the rogue wave on the background of the periodic standing wave. Instead, our solution describes an algebraic soliton traveling on the background of the periodic standing wave. This solution is similar to the solutions obtained on the dn-periodic wave in the mKdV equation [14]. We show that the exceptional curve coincides with the one obtained in [17] from the condition that the modulation instability band in the linearization of the focusing NLS equation (1.1) at the periodic standing wave is tangential to the imaginary axis at the origin of the complex plane.

Fifth, we visualize numerically the Lax spectrum, the admissible eigenvalues, the modulation instability bands, and the rogue waves.

The article is organized as follows. Section 2 describes the algebraic method with one eigenvalue which is used to relate the periodic standing waves with the eigenvalues in their Lax spectrum.

Section 3 characterizes parameters of the periodic standing waves and their representation in terms of the Jacobian elliptic functions. Section 4 characterizes the periodic and linearly growing solutions of the Lax equations at eigenvalues of the Lax spectrum related to the periodic standing waves. Section 5 presents exact expressions for the rogue waves and for their magnification factors. Section 6 discusses the relation between the existence of such rogue waves and the modulation instability bands for the periodic standing waves. Appendix A gives details of numerical computations of the Lax spectrum for the periodic standing waves. Appendix B contains technical details of computations involving Jacobian elliptic functions.

2. ALGEBRAIC METHOD WITH ONE EIGENVALUE

The NLS equation (1.1) with $\psi \equiv u$ appears as a compatibility condition $\varphi_{xt} = \varphi_{tx}$ of the following pair of linear equations on $\varphi \in \mathbb{C}^2$:

$$(2.1) \quad \varphi_x = Q(\lambda, u)\varphi, \quad Q(\lambda, u) = \begin{pmatrix} \lambda & u \\ -\bar{u} & -\lambda \end{pmatrix}$$

and

$$(2.2) \quad \varphi_t = S(\lambda, u)\varphi, \quad S(\lambda, u) = i \begin{pmatrix} \lambda^2 + \frac{1}{2}|u|^2 & \frac{1}{2}u_x + \lambda u \\ \frac{1}{2}\bar{u}_x - \lambda\bar{u} & -\lambda^2 - \frac{1}{2}|u|^2 \end{pmatrix},$$

where \bar{u} is the conjugate of u and $\lambda \in \mathbb{C}$ is a spectral parameter.

The procedure of computing a new solution $\psi \equiv \hat{u}$ of the NLS equation (1.1) from another solution $\psi \equiv u$ is well-known [4, 15, 21]. Let $\varphi = (p_1, q_1)^t$ be any nonzero solution to the linear equations (2.1) and (2.2) for a fixed value $\lambda = \lambda_1$. The new solution is given by the one-fold Darboux transformation

$$(2.3) \quad \hat{u} = u + \frac{2(\lambda_1 + \bar{\lambda}_1)p_1\bar{q}_1}{|p_1|^2 + |q_1|^2},$$

and in particular, it may represent a rogue wave \hat{u} on the background u satisfying the limits (1.4). The main question is which value λ_1 to fix and which nonzero solution φ to the linear equations (2.1)–(2.2) to take. It is clear from (2.3) that $\lambda_1 \notin i\mathbb{R}$, because if $\lambda_1 + \bar{\lambda}_1 = 0$, then $\hat{u} = u$. For the periodic standing wave in the form (1.3), we show that the admissible values of λ_1 are defined by the algebraic method with one eigenvalue, which is a particular case of a general method of nonlinearization of the linear equations on φ developed in [13] and [31, 32].

Let $\varphi = (p_1, q_1)^t$ be a nonzero solution of the linear equations (2.1)–(2.2) with fixed $\lambda = \lambda_1$ such that $\lambda_1 + \bar{\lambda}_1 \neq 0$. We introduce the following relation between the solution u to the NLS equation (1.1) and the squared eigenfunction $\varphi = (p_1, q_1)^t$:

$$(2.4) \quad u = p_1^2 + \bar{q}_1^2.$$

We intend to determine the value of λ_1 for which the relation (2.4) holds in (x, t) .

Assuming (2.4), the spectral problem (2.1) is nonlinearized into the following Hamiltonian system:

$$(2.5) \quad \frac{dp_1}{dx} = \frac{\partial H}{\partial q_1}, \quad \frac{dq_1}{dx} = -\frac{\partial H}{\partial p_1},$$

where the Hamiltonian function is

$$(2.6) \quad H = \lambda_1 p_1 q_1 + \bar{\lambda}_1 \bar{p}_1 \bar{q}_1 + \frac{1}{2}|p_1^2 + \bar{q}_1^2|^2$$

and the ordinary derivatives in x (at fixed t) are intentionally used in (2.5) to emphasize that the Hamiltonian system in x (at fixed t) is of degree two. The value of H is a constant of motion for the Hamiltonian system (2.5) together with another constant of motion:

$$(2.7) \quad F = i(p_1 q_1 - \bar{p}_1 \bar{q}_1).$$

Hence, the Hamiltonian system of degree two is Liouville integrable.

Assuming (2.4), the time-evolution problem (2.2) is nonlinearized into another Hamiltonian system given by

$$(2.8) \quad \frac{dp_1}{dt} = \frac{\partial K}{\partial q_1}, \quad \frac{dq_1}{dt} = -\frac{\partial K}{\partial p_1},$$

where the Hamiltonian function is

$$(2.9) \quad \begin{aligned} K = & i [2\lambda_1^2 p_1 q_1 - 2\bar{\lambda}_1^2 \bar{p}_1 \bar{q}_1 + |p_1^2 + \bar{q}_1^2|^2 (p_1 q_1 - \bar{p}_1 \bar{q}_1) \\ & + (\lambda_1 p_1^2 - \bar{\lambda}_1 \bar{q}_1^2)(\bar{p}_1^2 + q_1^2) + (p_1^2 + \bar{q}_1^2)(\lambda_1 q_1^2 - \bar{\lambda}_1 \bar{p}_1^2)] \end{aligned}$$

and the ordinary derivatives in t (at fixed x) are intentionally used in (2.8) to emphasize that the Hamiltonian system in t (at fixed x) is of degree two. The Hamiltonian system (2.8) is also Liouville integrable because both K in (2.9) and F in (2.7) are constant in t , where the latter conservation can be verified directly as follows:

$$\begin{aligned} \frac{dF}{dt} &= -q_1 [(2\lambda_1^2 + |u|^2)p_1 + (u_x + 2\lambda_1 u)q_1] - p_1 [-(2\lambda_1^2 + |u|^2)q_1 + (\bar{u}_x - 2\lambda_1 \bar{u})p_1] \\ &\quad - \bar{q}_1 [(2\bar{\lambda}_1^2 + |\bar{u}|^2)\bar{p}_1 + (\bar{u}_x + 2\bar{\lambda}_1 \bar{u})\bar{q}_1] - \bar{p}_1 [-(2\bar{\lambda}_1^2 + |\bar{u}|^2)\bar{q}_1 + (u_x - 2\bar{\lambda}_1 u)\bar{p}_1] \\ &= -[\bar{u}u_x + u\bar{u}_x + 2u(\lambda_1 q_1^2 - \bar{\lambda}_1 \bar{p}_1^2) + 2\bar{u}(\bar{\lambda}_1 \bar{q}_1^2 - \lambda_1^2 p_1^2)] \\ &= 0, \end{aligned}$$

thanks to the constraint that follows from differentiating (2.4) in x and substituting (2.5):

$$(2.10) \quad u_x = 2(\lambda_1 p_1^2 - \bar{\lambda}_1 \bar{q}_1^2) + 2(p_1^2 + \bar{q}_1^2)(p_1 q_1 - \bar{p}_1 \bar{q}_1).$$

Similarly, we can check that the Hamiltonian systems (2.5) and (2.8) commute in the sense of $\{H, K\} = 0$, where the Poisson bracket is given by

$$\{f, g\} := \frac{\partial f}{\partial p_1} \frac{\partial g}{\partial q_1} - \frac{\partial f}{\partial q_1} \frac{\partial g}{\partial p_1} + \frac{\partial f}{\partial \bar{p}_1} \frac{\partial g}{\partial \bar{q}_1} - \frac{\partial f}{\partial \bar{q}_1} \frac{\partial g}{\partial \bar{p}_1}.$$

It follows from (2.6), (2.9), and (2.10) that

$$\begin{aligned} \{H, K\} &= i [(\lambda_1 q_1 + \bar{u} p_1)((2\lambda_1^2 + |u|^2)p_1 + (u_x + 2\lambda_1 u)q_1) \\ &\quad + (\lambda_1 p_1 + u q_1)((\bar{u}_x - 2\lambda_1 \bar{u})p_1 - (2\lambda_1^2 + |u|^2)q_1) \\ &\quad - (\bar{\lambda}_1 \bar{q}_1 + u \bar{p}_1)((2\bar{\lambda}_1^2 + |\bar{u}|^2)\bar{p}_1 + (\bar{u}_x + 2\bar{\lambda}_1 \bar{u})\bar{q}_1) \\ &\quad - (\bar{\lambda}_1 \bar{p}_1 + \bar{u} \bar{q}_1)((u_x - 2\bar{\lambda}_1 u)\bar{p}_1 - (2\bar{\lambda}_1^2 + |\bar{u}|^2)\bar{q}_1)] \\ &= i [\lambda_1(u_x q_1^2 + \bar{u}_x p_1^2) - \bar{\lambda}_1(\bar{u}_x \bar{q}_1^2 + u_x \bar{p}_1^2) + (\bar{u}u_x + \bar{u}_x u)(p_1 q_1 - \bar{p}_1 \bar{q}_1)] \\ &= i [u_x(\lambda_1 q_1^2 - \bar{\lambda}_1 \bar{p}_1^2) + \bar{u}(p_1 q_1 - \bar{p}_1 \bar{q}_1) + \bar{u}_x(\lambda_1 p_1^2 - \bar{\lambda}_1 \bar{q}_1^2) + u(p_1 q_1 - \bar{p}_1 \bar{q}_1)] \\ &= 0. \end{aligned}$$

Since H and K commute, then H is constant in t and K is constant in x .

We claim and show next that the constraint (2.4) can only represent the class of standing and traveling wave solutions of the NLS equation (1.1) in the form

$$(2.11) \quad \psi(x, t) \equiv u(x, t) = U(x + ct)e^{2ibt},$$

where U is a complex-valued function and (c, b) are real-valued parameters. For the standing and traveling wave solution of the form (2.11), the constraint (2.4) determines solutions of the Hamiltonian systems (2.5) and (2.8) in the form

$$(2.12) \quad p_1(x, t) = P_1(x + ct)e^{ibt}, \quad q_1(x, t) = Q_1(x + ct)e^{-ibt},$$

where P_1 and Q_1 are complex-valued functions. Thanks to the commutativity of the Hamiltonian systems (2.5) and (2.8), this implies that the time evolution of $u(x, t)$, $p_1(x, t)$, and $q_1(x, t)$ in t is trivially given by (2.11) and (2.12), whereas the functional dependence of $u(x, t)$, $p_1(x, t)$, and $q_1(x, t)$ on x is non-trivial. Due to this reason, we abuse the notations and only refer to the x -dependence of u , p_1 , and q_1 in what follows before Section 4. In particular, we rewrite (2.10) in the equivalent form:

$$(2.13) \quad \frac{du}{dx} + 2iFu = 2(\lambda_1 p_1^2 - \bar{\lambda}_1 \bar{q}_1^2),$$

where the ordinary derivative in x is now used. By differentiating (2.13) and using (2.5), (2.6), and (2.7), we obtain

$$(2.14) \quad \frac{d^2 u}{dx^2} + 2|u|^2 u + 2iF \frac{du}{dx} - 4Hu = 4(\lambda_1^2 p_1^2 + \bar{\lambda}_1^2 \bar{q}_1^2).$$

Eliminating the squared eigenfunctions p_1^2 and \bar{q}_1^2 from (2.4) and (2.13) and substituting the result into (2.14) yields a closed second-order equation:

$$(2.15) \quad \frac{d^2 u}{dx^2} + 2|u|^2 u + 2ic \frac{du}{dx} - 4bu = 0,$$

where c and b are real parameters given by

$$(2.16) \quad \begin{cases} c = F + i(\lambda_1 - \bar{\lambda}_1), \\ b = H + iF(\lambda_1 - \bar{\lambda}_1) + |\lambda_1|^2. \end{cases}$$

The differential equation (2.15) is a standing and traveling wave reduction of the NLS equation (1.1) for the solutions in the form (2.11) with $u \equiv U$. Hence, the constraint (2.4) can only represent the class of standing and traveling wave solutions of the NLS equation (1.1).

In order to complete the algebraic method with one eigenvalue and to integrate the second-order equation (2.15), we represent the Hamiltonian system (2.5) by using the following Lax equation:

$$(2.17) \quad \frac{d}{dx} W(\lambda) = [Q(\lambda, u), W(\lambda)],$$

where $Q(\lambda, u)$ is given by (2.1), u is given by (2.4), and $W(\lambda)$ is represented in the form:

$$(2.18) \quad W(\lambda) = \begin{pmatrix} W_{11}(\lambda) & W_{12}(\lambda) \\ \bar{W}_{12}(-\lambda) & -\bar{W}_{11}(-\lambda) \end{pmatrix},$$

with the entries

$$(2.19) \quad W_{11}(\lambda) = 1 - \left(\frac{p_1 q_1}{\lambda - \lambda_1} - \frac{\bar{p}_1 \bar{q}_1}{\lambda + \bar{\lambda}_1} \right), \quad W_{12}(\lambda) = \frac{p_1^2}{\lambda - \lambda_1} + \frac{\bar{q}_1^2}{\lambda + \bar{\lambda}_1}.$$

By using (2.4), (2.6), (2.7), and (2.13), we can rewrite the pole decompositions (2.19) in the form:

$$(2.20) \quad W_{11}(\lambda) = \frac{\lambda^2 + ic\lambda + \frac{1}{2}|u|^2 - b}{(\lambda - \lambda_1)(\lambda + \bar{\lambda}_1)}, \quad W_{12}(\lambda) = \frac{u\lambda + \frac{1}{2}\frac{du}{dx} + icu}{(\lambda - \lambda_1)(\lambda + \bar{\lambda}_1)}.$$

It follows from (2.18) and (2.19) that

$$(2.21) \quad \det W(\lambda) = -[W_{11}(\lambda)]^2 - W_{12}(\lambda)\bar{W}_{12}(-\lambda)$$

can be reduced with the help of (2.6) and (2.7) to the form

$$(2.22) \quad \det W(\lambda) = -1 + \frac{2[H - iF(\lambda - \lambda_1 + \bar{\lambda}_1)]}{(\lambda - \lambda_1)(\lambda + \bar{\lambda}_1)}.$$

This expression proves that $\det W(\lambda)$ contains only simple poles at λ_1 and $-\bar{\lambda}_1$ and that $\det W(\lambda)$ is constant in (x, t) . Moreover, if $\lambda_1 + \bar{\lambda}_1 \neq 0$ and $(H, F) \neq (0, 0)$, then the residue terms at λ_1 and $-\bar{\lambda}_1$ are nonzero.

The $(1, 2)$ -component of the Lax equation (2.17) with (2.18) and (2.20) is equivalent to the second-order equation (2.15). On the other hand, the first-order invariants for the second-order equation (2.15) follow from the properties of $\det W(\lambda)$. By using (2.18) and (2.20), we obtain

$$(2.23) \quad \det W(\lambda) = -\frac{P(\lambda)}{(\lambda - \lambda_1)^2(\lambda + \bar{\lambda}_1)^2},$$

where

$$(2.24) \quad P(\lambda) := \left(\lambda^2 + ic\lambda + \frac{1}{2}|u|^2 - b \right)^2 - \left(u\lambda + \frac{1}{2}\frac{du}{dx} + icu \right) \left(\bar{u}\lambda - \frac{1}{2}\frac{d\bar{u}}{dx} + ic\bar{u} \right).$$

Since $P(\lambda)$ is independent of (x, t) , expanding the polynomial $P(\lambda)$ in powers of λ gives two first-order invariants for the second-order equation (2.15) in the form:

$$(2.25) \quad \left| \frac{du}{dx} \right|^2 + |u|^4 - 4b|u|^2 = 8d$$

and

$$(2.26) \quad i \left(\frac{du}{dx} \bar{u} - u \frac{d\bar{u}}{dx} \right) - 2c|u|^2 = 4a$$

where d and a are real parameters appearing in the coefficients of the polynomial $P(\lambda)$ given by

$$(2.27) \quad P(\lambda) = \lambda^4 + 2ic\lambda^3 - (c^2 + 2b)\lambda^2 + 2i(a - bc)\lambda + b^2 - 2ac + 2d.$$

If λ_1 is a root of $P(\lambda)$, so is $-\bar{\lambda}_1$, thanks to the symmetry of the coefficients in $P(\lambda)$. The admissible values for λ_1 are given by four roots of $P(\lambda)$ which are symmetric about the imaginary axis. If λ_1 is a simple root of $P(\lambda)$, then $\det W(\lambda)$ has simple poles at λ_1 and $-\bar{\lambda}_1$ in the quotient (2.21). Since the residue terms in (2.21) are nonzero if $\lambda_1 + \bar{\lambda}_1 \neq 0$ and $(H, F) \neq (0, 0)$, it is clear that λ_1 cannot be a double root of $P(\lambda)$.

3. CLASSIFICATION OF PERIODIC STANDING WAVES

Here we solve the second-order equation (2.15) by using Jacobian elliptic functions. The algebraic method with one eigenvalue allows us to define the admissible values of λ_1 for the periodic standing waves of the NLS equation (1.1).

First, we note that the transformation

$$(3.1) \quad u(x) = \tilde{u}(x)e^{-icx}, \quad b = \tilde{b} + \frac{1}{4}c^2, \quad d = \tilde{d} + \frac{1}{2}ac, \quad a = \tilde{a}$$

leaves the system (2.15), (2.25) and (2.26) invariant for tilde variables and eliminates the parameter c . Similarly, $P(\lambda)$ in (2.27) can be written as

$$(3.2) \quad P(\lambda) = \left(\lambda + \frac{i}{2}c \right)^4 - 2\tilde{b} \left(\lambda + \frac{i}{2}c \right)^2 + 2i\tilde{a} \left(\lambda + \frac{i}{2}c \right) + \tilde{b}^2 + 2\tilde{d},$$

which shows that the dependence of $P(\lambda)$ on c can be scaled out by a translation in the spectral plane of λ . Hence, one can set $c = 0$ without loss of generality. This corresponds to the Lorentz transformation which generates a standing and traveling wave solution of the NLS equation (1.1) in the form (2.11) from every standing wave solution in the form (1.3).

The periodic standing waves are divided into two groups depending on whether the phase of the complex-valued function $u(x)$ is trivial or non-trivial.

3.1. Periodic standing waves with trivial phase. Let us set $c = 0$ and $a = 0$, where the first choice is made without loss of generality thanks to the transformations (3.1) and (3.2), whereas the second choice trivializes the phase and simplifies the construction of periodic standing waves in Jacobian elliptic functions. It follows from (2.26) with $c = a = 0$ that

$$\frac{d}{dx} \log \left(\frac{u}{\bar{u}} \right) = 0 \quad \Rightarrow \quad \frac{u}{\bar{u}} = e^{2i\theta},$$

where real θ is constant in x . Thanks to the rotational symmetry of solutions to the NLS equation (1.1), one can take $u(x)$ as a real function. The first-order quadrature (2.25) is rewritten for real $u(x)$ as follows:

$$(3.3) \quad \left(\frac{du}{dx} \right)^2 + V(u) = 0, \quad V(u) := u^4 - 4bu^2 - 8d.$$

The four roots of $V(u)$ are symmetric and can be enumerated as $\pm u_1$ and $\pm u_2$. If all four roots are real, one can order them as

$$(3.4) \quad -u_1 \leq -u_2 \leq 0 \leq u_2 \leq u_1.$$

Solutions of the first-order quadrature (3.3) exist either in $[-u_1, -u_2]$ or in $[u_2, u_1]$. The two solutions are related by the transformation $u \mapsto -u$, hence without loss of generality, one can consider the positive solution in $[u_2, u_1]$. This solution is given by the explicit formula

$$(3.5) \quad u(x) = u_1 \operatorname{dn}(u_1 x; k), \quad k := \frac{\sqrt{u_1^2 - u_2^2}}{u_1}.$$

If two roots of $V(u)$ are real (e.g., $\pm u_1$) and two roots are complex (e.g., $\pm u_2 = \pm i\nu_2$), the solution in $[-u_1, u_1]$ is given by the explicit formula

$$(3.6) \quad u(x) = u_1 \operatorname{cn}(\alpha x; k), \quad \alpha := \sqrt{u_1^2 + \nu_2^2}, \quad k := \frac{u_1}{\sqrt{u_1^2 + \nu_2^2}}.$$

The connection formulas of roots $\pm u_1, \pm u_2$ with the parameters (b, d) in (3.3) are given by

$$(3.7) \quad \begin{cases} 4b = u_1^2 + u_2^2, \\ 8d = -u_1^2 u_2^2. \end{cases}$$

Substituting (3.7) into $P(\lambda)$ given by (2.27) with $c = a = 0$ yields

$$(3.8) \quad P(\lambda) = \lambda^4 - \frac{1}{2}(u_1^2 + u_2^2)\lambda^2 + \frac{1}{16}(u_1^2 - u_2^2)^2.$$

The two admissible pairs of eigenvalues are given by

$$(3.9) \quad \lambda_1^\pm = \pm \frac{u_1 + u_2}{2}, \quad \lambda_2^\pm = \pm \frac{u_1 - u_2}{2},$$

where u_1 is real and u_2 is either real for (3.5) or purely imaginary for (3.6).

Both waves with the trivial phase can be simplified by using the scaling transformation of solutions to the NLS equation (1.1):

$$(3.10) \quad \text{if } u(x, t) \text{ is a solution, so is } au(ax, a^2 t), \text{ for every } a \in \mathbb{R}.$$

The dn-periodic wave (3.5) with $u_1 = 1$ and $u_2 = \sqrt{1 - k^2}$ becomes

$$(3.11) \quad u(x) = \operatorname{dn}(x; k), \quad k \in (0, 1)$$

and the two eigenvalue pairs in (3.9) are real-valued:

$$(3.12) \quad \lambda_1^\pm = \pm \frac{1}{2}(1 + \sqrt{1 - k^2}), \quad \lambda_2^\pm = \pm \frac{1}{2}(1 - \sqrt{1 - k^2}).$$

The cn-periodic wave (3.6) with $u_1 = k$ and $\nu_2 = \sqrt{1 - k^2}$ becomes

$$(3.13) \quad u(x) = k \operatorname{cn}(x; k), \quad k \in (0, 1)$$

and the two eigenvalue pairs in (3.9) form a complex quadruplet:

$$(3.14) \quad \lambda_1^\pm = \frac{1}{2}(\pm k + i\sqrt{1 - k^2}), \quad \lambda_2^\pm = \frac{1}{2}(\pm k - i\sqrt{1 - k^2}).$$

These two cases agree with the outcomes of the algebraic method in [15] and with the explicit expressions obtained in [24].

Figs. 1 and 2 represent the Lax spectrum computed numerically by using the Floquet–Bloch decomposition of solutions to the spectral problem (2.1) with the potentials u in the form (3.11) and (3.13) respectively. The black curves represent the purely continuous spectrum whereas the red dots represent eigenvalues (3.12) and (3.14) respectively. Appendix A gives details of the Floquet–Bloch decomposition and the numerical method used to compute the Lax spectrum at the periodic standing waves.

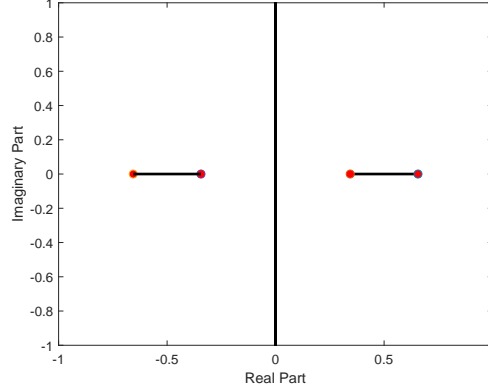


FIGURE 1. Lax spectrum for the dn-periodic wave (3.11) with $k = 0.95$. Red dots represent eigenvalues (3.12).

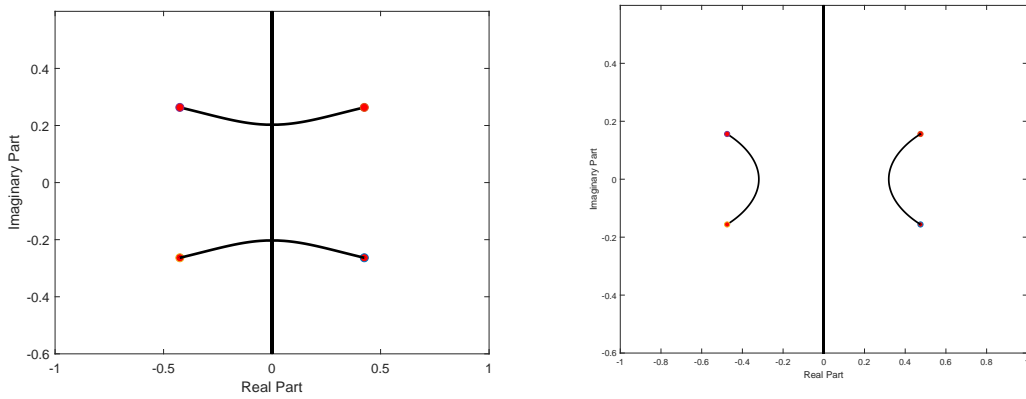


FIGURE 2. Lax spectrum for the cn-periodic wave (3.13) with $k = 0.85$ (left) and $k = 0.95$ (right). Red dots represent eigenvalues (3.14).

3.2. Periodic standing waves with nontrivial phase. Let us set $c = 0$ but consider $a \neq 0$. Substituting the decomposition $u(x) = R(x)e^{i\Theta(x)}$ with real R and Θ into (2.25) and (2.26) with $c = 0$ yields the system of first-order equations:

$$(3.15) \quad \begin{cases} \left(\frac{dR}{dx}\right)^2 + R^2 \left(\frac{d\Theta}{dx}\right)^2 + R^4 - 4bR^2 = 8d, \\ R^2 \frac{d\Theta}{dx} = -2a. \end{cases}$$

Substituting $\frac{d\Theta}{dx}$ from the second equation to the first equation results in the following first-order quadrature:

$$(3.16) \quad \left(\frac{dR}{dx}\right)^2 + 4a^2 R^{-2} + R^4 - 4bR^2 = 8d.$$

The singularity $R = 0$ is unfolded with the transformation $\rho = R^2$ which yields

$$(3.17) \quad \frac{1}{4} \left(\frac{d\rho}{dx}\right)^2 + Z(\rho) = 0, \quad Z(\rho) := \rho^3 - 4b\rho^2 - 8d\rho + 4a^2.$$

Since $\rho = R^2 \geq 0$ and $Z(0) = 4a^2 \geq 0$, one of the roots of the cubic polynomial Z is negative. Therefore, the positive periodic solutions of the first-order quadrature (3.17) exist only if there exist three real roots of Z . We denote the roots by $\{\rho_1, \rho_2, \rho_3\}$ and order them as follows:

$$(3.18) \quad \rho_3 \leq 0 \leq \rho_2 \leq \rho_1.$$

The connection formulas of roots ρ_1 , ρ_2 , and ρ_3 to the parameters (b, d) in (3.3) are given by

$$(3.19) \quad \begin{cases} 4b = \rho_1 + \rho_2 + \rho_3, \\ 8d = -\rho_1\rho_2 - \rho_1\rho_3 - \rho_2\rho_3, \\ 4a^2 = -\rho_1\rho_2\rho_3. \end{cases}$$

Only one square root for a must be used for a particular periodic standing wave. In what follows, we shall use the negative square root with $2a = -\sqrt{\rho_1\rho_2}\sqrt{-\rho_3}$, which is real-valued thanks to (3.18).

The positive periodic solution is located in the interval $[\rho_2, \rho_1]$ and is given by

$$(3.20) \quad \rho(x) = \rho_1 - (\rho_1 - \rho_2)\text{sn}^2(\alpha x; k),$$

where α and k are related to (ρ_1, ρ_2, ρ_3) by

$$(3.21) \quad \alpha^2 = \rho_1 - \rho_3, \quad k^2 = \frac{\rho_1 - \rho_2}{\rho_1 - \rho_3}.$$

Thanks to the scaling transformation (3.10), we can set $\alpha = 1$ and use the parametrization $\rho_1 = \beta$, $\rho_2 = \beta - k^2$, and $\rho_3 = \beta - 1$ which yields the exact expression considered in [17]:

$$(3.22) \quad \rho(x) = \beta - k^2 \text{sn}^2(x; k).$$

The exact solution (3.22) has two parameters β and k which belong to the following triangular region: $k \in [0, 1]$ (since $\rho_3 \leq \rho_2 \leq \rho_1$), $\beta \leq 1$ (since $\rho_3 \leq 0$), and $\beta \geq k^2$ (since $\rho_2 \geq 0$). On the three boundaries, we have reductions to the dn-periodic wave (3.11) if $\beta = 1$ ($\rho_3 = 0$), the cn-periodic wave (3.13) if $\beta = k^2$ ($\rho_2 = 0$), and the constant-amplitude wave if $k = 0$ ($\rho_1 = \rho_2$):

$$(3.23) \quad u(x) = \sqrt{\beta} e^{i\sqrt{1-\beta}x}, \quad \beta \in (0, 1).$$

Substituting (3.19) into $P(\lambda)$ given by (2.27) with $c = 0$ yields

$$(3.24) \quad P(\lambda) = \lambda^4 - \frac{1}{2}(\rho_1 + \rho_2 + \rho_3)\lambda^2 - i\sqrt{\rho_1\rho_2}\sqrt{-\rho_3}\lambda + \frac{1}{16}(\rho_1^2 + \rho_2^2 + \rho_3^2 - 2\rho_1\rho_2 - 2\rho_1\rho_3 - 2\rho_2\rho_3).$$

The four roots of $P(\lambda)$ can now be found in the explicit form:

$$(3.25) \quad \lambda_1^\pm = \pm \frac{1}{2}(\sqrt{\rho_1} + \sqrt{\rho_2}) + \frac{i}{2}\sqrt{-\rho_3}, \quad \lambda_2^\pm = \pm \frac{1}{2}(\sqrt{\rho_1} - \sqrt{\rho_2}) - \frac{i}{2}\sqrt{-\rho_3},$$

which was stated in equation (88) in [17] without a proof.

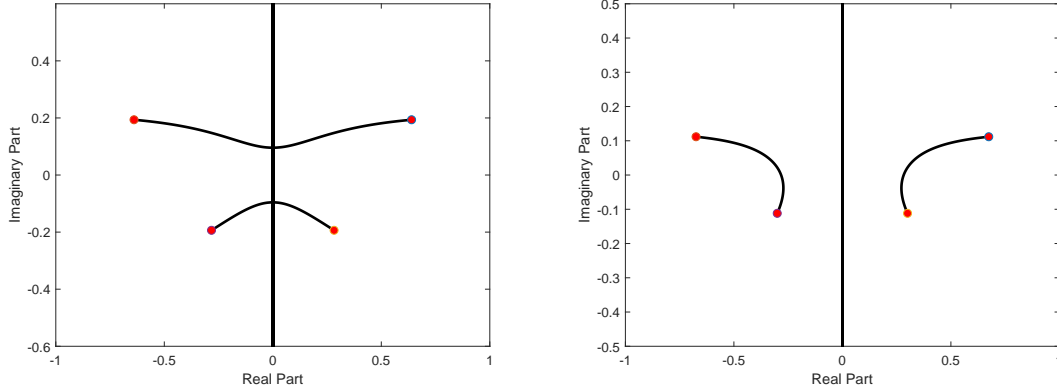


FIGURE 3. Lax spectrum for the periodic wave (3.22) with $(\beta, k) = (0.85, 0.85)$ (left) and $(\beta, k) = (0.95, 0.9)$ (right). Red dots represent eigenvalues (3.25).

Fig. 3 represents the Lax spectrum computed numerically by using the Floquet–Bloch decomposition of solutions to the spectral problem (2.1) with the potentials given by $u(x) = R(x)e^{i\Theta(x)}$. The transformation

$$(3.26) \quad p_1(x) = \tilde{p}_1(x)e^{i\Theta(x)/2}, \quad q_1(x) = \tilde{q}_1(x)e^{-i\Theta(x)/2}$$

is used to reduce the spectral problem (2.1) to the one with a periodic potential considered in Appendix A. Note that the transformation (3.26) affects the eigenfunctions but preserves the eigenvalues λ in the spectral problem (2.1). The black curves on Fig. 3 represent the purely continuous spectrum whereas the red dots represent eigenvalues (3.25).

Fig. 4 shows boundaries of the triangular region on the (β, k) plane where the periodic waves with nontrivial phase exist (black curves). Blue dots represent the particular values of parameters (β, k) chosen for illustration of the Lax spectrum on Figs. 1, 2, and 3. The green curve given by the following explicit expression (see equation (100) in [17])

$$(3.27) \quad \beta = -1 + k^2 + \frac{2E(k)}{K(k)},$$

separates two regions on the (β, k) plane. The Lax spectrum for the periodic waves in the lower (upper) region includes bands crossing the imaginary (real) axis. The two choices on Figs. 2 and 3 correspond to two points on both sides of the boundary (3.27) on Fig. 4.

4. EIGENFUNCTIONS OF THE LINEAR EQUATIONS

Here we characterize squared eigenfunctions of the linear equations (2.1)–(2.2) in terms of the periodic standing wave u . For each admissible eigenvalue λ_1 among the roots of the polynomial $P(\lambda)$ in (2.27), the squared eigenfunctions p_1^2 , \bar{q}_1^2 , and p_1q_1 after the transformation (3.26) are periodic functions with the same period as the periodic wave u . The second linearly independent solution of the linear equations (2.1)–(2.2) exists for the same eigenvalues and is characterized in terms of the periodic eigenfunctions. The second solution is not periodic and grows linearly in x and t almost everywhere on the (x, t) -plane.

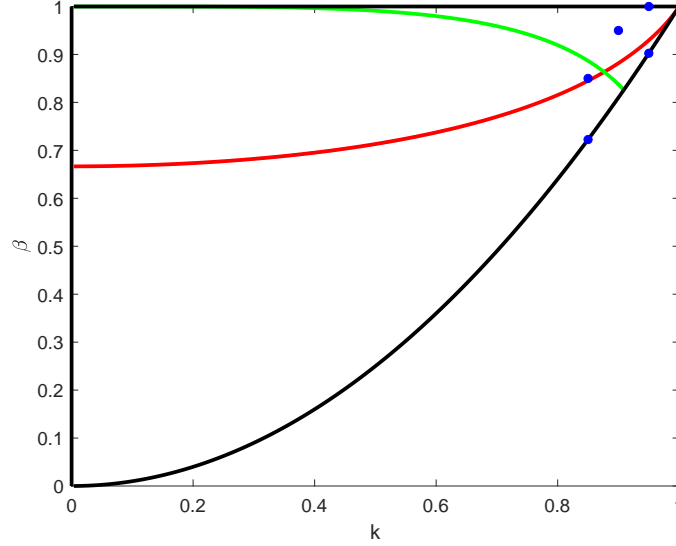


FIGURE 4. The black curves are boundaries of the triangular region where the periodic waves with nontrivial phase exist. The blue dots show parameter values of (β, k) for the solutions chosen for illustration on Figs. 1, 2, and 3. The green curve displays the boundary (3.27), whereas the red curve shows the boundary (4.23).

Let us recall the representations (2.19) and (2.20) for $W_{11}(\lambda)$ and $W_{12}(\lambda)$ in terms of the squared eigenfunctions for (2.19) and the periodic standing wave u for (2.20). By evaluating the residue terms at simple poles $\lambda = \lambda_1$ and $\lambda = -\bar{\lambda}_1$ in each representation (2.19) and (2.20), we obtain the following explicit expressions for p_1^2 , \bar{q}_1^2 , and $p_1 q_1$:

$$(4.1) \quad \begin{cases} p_1^2 = \frac{1}{\lambda_1 + \bar{\lambda}_1} \left[\frac{1}{2} \frac{du}{dx} + icu + \lambda_1 u \right], \\ \bar{q}_1^2 = \frac{1}{\lambda_1 + \bar{\lambda}_1} \left[-\frac{1}{2} \frac{du}{dx} - icu + \bar{\lambda}_1 u \right], \\ p_1 q_1 = -\frac{1}{\lambda_1 + \bar{\lambda}_1} \left[\frac{1}{2} |u|^2 - b + i\lambda_1 c + \lambda_1^2 \right]. \end{cases}$$

Let $\varphi = (p_1, q_1)^T$ be a solution of the linear equations (2.1)–(2.2) for $\lambda = \lambda_1$. If u is a L -periodic standing wave, then p_1^2 and q_1^2 is periodic with the same period L in x after the transformation (3.26). The second, linearly independent solution $\varphi = (\hat{p}_1, \hat{q}_1)^T$ of the same equations (2.1)–(2.2) for $\lambda = \lambda_1$ can be written in the form:

$$(4.2) \quad \hat{p}_1 = p_1 \phi_1 - \frac{2\bar{q}_1}{|p_1|^2 + |q_1|^2}, \quad \hat{q}_1 = q_1 \phi_1 + \frac{2\bar{p}_1}{|p_1|^2 + |q_1|^2},$$

where ϕ_1 is to be determined as a function of (x, t) . Wronskian between the two solutions is normalized by $p_1 \hat{q}_1 - \hat{p}_1 q_1 = 2$. Note that if u is the periodic standing wave in the form

$$(4.3) \quad u(x, t) = U(x) e^{2ibt},$$

then the first solution $\varphi = (p_1, q_1)^T$ to the linear equations (2.1)–(2.2) for $\lambda = \lambda_1$ is written in the form

$$(4.4) \quad p_1(x, t) = P_1(x) e^{ibt}, \quad q_1(x, t) = Q_1(x) e^{-ibt},$$

whereas the second solution $\varphi = (\hat{p}_1, \hat{q}_1)^T$ to the same equations is written in the form

$$(4.5) \quad \hat{p}_1(x, t) = \hat{P}_1(x, t) e^{ibt}, \quad \hat{q}_1(x, t) = \hat{Q}_1(x, t) e^{-ibt},$$

where $\hat{P}_1(x, t)$ and $\hat{Q}_1(x, t)$ depend on t only through the function $\phi_1(x, t)$.

Substituting (4.2) into (2.1) and using (2.1) for $\varphi = (p_1, q_1)^T$ yields the following equation for ϕ_1 :

$$(4.6) \quad \frac{\partial \phi_1}{\partial x} = -\frac{4(\lambda_1 + \bar{\lambda}_1)\bar{p}_1\bar{q}_1}{(|p_1|^2 + |q_1|^2)^2}.$$

Similarly, substituting (4.2) into (2.2) and using (2.2) for $\varphi = (p_1, q_1)^T$ yields another equation for ϕ_1 :

$$(4.7) \quad \frac{\partial \phi_1}{\partial t} = -\frac{4i(\lambda_1^2 - \bar{\lambda}_1^2)\bar{p}_1\bar{q}_1}{(|p_1|^2 + |q_1|^2)^2} + \frac{2i(\lambda_1 + \bar{\lambda}_1)(u\bar{p}_1^2 + \bar{u}\bar{q}_1^2)}{(|p_1|^2 + |q_1|^2)^2}.$$

The system of first-order equations (4.6) and (4.7) is compatible in the sense $\phi_{1xt} = \phi_{1tx}$ since it is derived from the compatible Lax system (2.1)–(2.2). Note also that the transformation (4.4) leaves equations (4.6) and (4.7) invariant for $\phi_1(x, t)$.

4.1. Periodic standing waves with trivial phase. We set $c = a = 0$ in solutions of the system (2.15), (2.25), and (2.26). We also use the scaling transformation (3.10). There exist two admissible pairs of values of λ_1 given by (3.12) for the dn-periodic solution (3.11) and (3.14) for the cn-periodic solution (3.13). Let us fix

$$(4.8) \quad \lambda_1 = \frac{1}{2}(u_1 \pm u_2),$$

for two eigenvalues in either (3.12) or (3.14).

The periodic standing waves are written in the form (4.3) with real-valued U . By separating the variables in (4.4) and using $b = \frac{1}{4}(u_1^2 + u_2^2)$, we obtain

$$(4.9) \quad \begin{cases} P_1^2 = \frac{1}{\lambda_1 + \bar{\lambda}_1} \left(\frac{1}{2} \frac{dU}{dx} + \lambda_1 U \right), \\ \bar{Q}_1^2 = \frac{1}{\lambda_1 + \bar{\lambda}_1} \left(-\frac{1}{2} \frac{dU}{dx} + \bar{\lambda}_1 U \right), \\ P_1 Q_1 = -\frac{1}{2(\lambda_1 + \bar{\lambda}_1)} (\pm u_1 u_2 + U^2). \end{cases}$$

The quantities λ_1 , P_1 and Q_1 are real-valued for the dn-periodic wave (3.11). By using (4.9), we solve the first-order equations (4.6) and (4.7) in the closed form:

$$(4.10) \quad \phi_1(x, t) = 2x + 2i(1 \pm \sqrt{1 - k^2})t \pm 2\sqrt{1 - k^2} \int_0^x \frac{dy}{\text{dn}^2(y; k)}$$

up to addition of a complex-valued constant. We note that

$$(4.11) \quad K(k) \pm \sqrt{1 - k^2} \int_0^{K(k)} \frac{dy}{\text{dn}^2(y; k)} = K(k) \pm \frac{E(k)}{\sqrt{1 - k^2}} \gtrless 0, \quad k \in (0, 1),$$

where the inequality for the upper sign is trivial, whereas the inequality for the lower sign follows from the inequality 19.9.8 in [28], that is, from

$$(4.12) \quad \frac{E(k)}{K(k)} > \sqrt{1 - k^2}.$$

Thanks to (4.11), the function $\phi_1(x, t)$ grows linearly as $|x| + |t| \rightarrow \infty$ for both signs. Hence, the second solution $\varphi = (\hat{p}_1, \hat{q}_1)^T$ given by (4.2) with ϕ_1 in (4.10) grows linearly as $|x| + |t| \rightarrow \infty$ everywhere on the (x, t) -plane. Compared to the representation for $\varphi = (\hat{p}_1, \hat{q}_1)^T$ used in [15], the new representation (4.2) has the advantage of being equally applicable to both eigenvalues $\lambda_1 = \frac{1}{2}(u_1 \pm u_2)$ because the denominators in the new representation (4.2) with (4.10) never vanish.

For the cn-periodic wave (3.13), λ_1 is complex and so are P_1 and Q_1 . It was found in [15] that

$$(4.13) \quad |P_1(x)|^2 + |Q_1(x)|^2 = \text{dn}(x; k)$$

and

$$(4.14) \quad 2P_1(x)\bar{Q}_1(x) = -\text{cn}(x; k)\text{dn}(x; k) \mp i\sqrt{1-k^2}\text{sn}(x; k).$$

By using (4.9) and (4.13), we solve the first-order equations (4.6) and (4.7) in the closed form:

$$(4.15) \quad \phi_1(x, t) = 2k^2 \int_0^x \frac{\text{cn}^2(y; k)dy}{\text{dn}^2(y; k)} \mp 2ik\sqrt{1-k^2} \int_0^x \frac{dy}{\text{dn}^2(y; k)} + 2ikt$$

up to addition of a complex-valued constant. It is clear from (4.15) that $\phi_1(x, t)$ grows linearly as $|x| + |t| \rightarrow \infty$ for both signs in (4.15), hence, the second solution $\varphi = (\hat{p}_1, \hat{q}_1)^T$ given by (4.2) with ϕ_1 in (4.15) also grows linearly as $|x| + |t| \rightarrow \infty$ everywhere on the (x, t) -plane. Compared to the representation used in [15], it is now easier to see the growth of $\phi_1(x, t)$ at infinity.

4.2. Periodic standing waves with nontrivial phase. We set $c = 0$ for solutions of the system (2.15), (2.25), and (2.26). Let the roots $\{\rho_1, \rho_2, \rho_3\}$ satisfy the order (3.18). There exist two admissible pairs of values of λ_1 and they are given in the explicit form (3.25). Let us fix

$$(4.16) \quad \lambda_1 = \frac{1}{2}(\sqrt{\rho_1} \pm \sqrt{\rho_2}) \pm \frac{i}{2}\sqrt{-\rho_3}$$

for two eigenvalues in (3.25).

The periodic standing waves are given in the form (4.3) with complex-valued U . By separating the variables in (4.4) and using $b = \frac{1}{4}(\rho_1 + \rho_2 + \rho_3)$, we obtain

$$(4.17) \quad \begin{cases} P_1^2 = \frac{1}{\lambda_1 + \bar{\lambda}_1} \left(\frac{1}{2} \frac{dU}{dx} + \lambda_1 U \right), \\ \bar{Q}_1^2 = \frac{1}{\lambda_1 + \bar{\lambda}_1} \left(-\frac{1}{2} \frac{dU}{dx} + \bar{\lambda}_1 U \right), \\ P_1 Q_1 = -\frac{1}{2(\lambda_1 + \bar{\lambda}_1)} \left(\pm \sqrt{\rho_1 \rho_2} \pm i\sqrt{-\rho_3}(\sqrt{\rho_1} \pm \sqrt{\rho_2}) + |U|^2 \right). \end{cases}$$

Next, we represent the solutions in the polar form:

$$(4.18) \quad U(x) = R(x)e^{i\Theta(x)}, \quad P_1(x) = \tilde{P}_1(x)e^{i\Theta(x)/2}, \quad Q_1(x) = \tilde{Q}_1(x)e^{-i\Theta(x)/2},$$

where R and Θ are real, whereas \tilde{P}_1 and \tilde{Q}_1 are complex-valued. In Appendix B, we prove that

$$(4.19) \quad |\tilde{P}_1(x)|^2 + |\tilde{Q}_1(x)|^2 = \text{dn}(x; k)$$

and

$$(4.20) \quad \tilde{P}_1(x)\bar{\tilde{Q}}_1(x) = -\frac{1}{2(\sqrt{\rho_1} \pm \sqrt{\rho_2})} \left[\frac{\text{dn}(x; k)}{R(x)} (R(x)^2 \pm \sqrt{\rho_1 \rho_2}) \mp \frac{i\sqrt{-\rho_3}}{\text{dn}(x; k)} \frac{dR}{dx} \right].$$

By using (4.17) and (4.19), we solve the first-order equations (4.6) and (4.7) in the closed form:

$$(4.21) \quad \phi_1(x, t) = 2 \int_0^x \frac{\rho(y) \pm \sqrt{\rho_1 \rho_2} \mp i\sqrt{-\rho_3}(\sqrt{\rho_1} \pm \sqrt{\rho_2})}{\text{dn}^2(y; k)} dy + 2i(\sqrt{\rho_1} \pm \sqrt{\rho_2})t$$

up to addition of a complex-valued constant. When $\rho_1 = 1$, $\rho_2 = 1 - k^2$, and $\rho_3 = 0$, expression (4.21) is equivalent to (4.10) for the dn-periodic wave (3.11). When $\rho_1 = k^2$, $\rho_2 = 0$, and $\rho_3 = -(1 - k^2)$, expression (4.21) is equivalent to (4.15) for the cn-periodic wave (3.13).

It is clear from (4.21) with the upper sign that $\phi_1(x, t)$ grows linearly as $|x| + |t| \rightarrow \infty$. On the other hand, it follows from (4.21) with the lower sign that $\phi_1(x, t)$ does not grow everywhere as $|x| + |t| \rightarrow \infty$ if

$$(4.22) \quad \int_0^{K(k)} \frac{\rho(y) - \sqrt{\rho_1 \rho_2}}{\text{dn}^2(y; k)} dy = 0,$$

where the integral for ρ given by (3.22) can be evaluated in Jacobian elliptic integrals as follows:

$$(4.23) \quad K(k) + \frac{\beta - 1 - \sqrt{\beta(\beta - k^2)}}{1 - k^2} E(k) = 0.$$

If the constraint (4.22) is satisfied, then $\phi_1(x, t)$ is bounded as $|x| + |t| \rightarrow \infty$ along the family of straight lines

$$(4.24) \quad t + \sqrt{-\rho_3} \left[\int_0^{K(k)} \frac{dy}{\operatorname{dn}^2(y; k)} \right] \frac{x}{K(k)} = t_0,$$

where $t_0 \in \mathbb{R}$ is arbitrary.

We claim that there exists exactly one root of the constraint (4.23) in $\beta \in (k^2, 1)$ for every $k \in (0, 1)$. Indeed, we obtain

$$\begin{aligned} \beta = k^2 : \quad & K(k) + \frac{\beta - 1 - \sqrt{\beta(\beta - k^2)}}{1 - k^2} \Big|_{\beta=k^2} E(k) = K(k) - E(k) > 0, \\ \beta = 1 : \quad & K(k) + \frac{\beta - 1 - \sqrt{\beta(\beta - k^2)}}{1 - k^2} \Big|_{\beta=1} E(k) = K(k) - \frac{E(k)}{\sqrt{1 - k^2}} < 0, \end{aligned}$$

where the first inequality is due to 19.9.6 in [28] and the second inequality is due to (4.12). Since the left-hand side of (4.23) is a C^1 function of β in $(k^2, 1)$ for every $k \in (0, 1)$, there exists at least one $\beta \in (k^2, 1)$ such that constraint (4.23) is satisfied. Moreover, differentiating the left-hand side of (4.23) in β yields for $\beta \in [k^2, 1]$:

$$\frac{E(k)}{1 - k^2} \left[1 - \frac{\sqrt{\beta - k^2}}{2\sqrt{\beta}} - \frac{\sqrt{\beta}}{2\sqrt{\beta - k^2}} \right] = \frac{E(k)}{2(1 - k^2)\sqrt{\beta(\beta - k^2)}} \left[2\sqrt{\beta(\beta - k^2)} - \beta - (\beta - k^2) \right],$$

where the right-hand side is negative due to the Cauchy-Schwarz inequality. Hence, the left-hand side of (4.23) is decreasing in β and there is exactly one $\beta \in (k^2, 1)$ where the constraint (4.23) is satisfied. The red curve on Fig. 4 shows the only root of the constraint (4.23) on the (β, k) plane.

5. ROGUE WAVES ON THE PERIODIC BACKGROUND

Here we use the one-fold Darboux transformation (2.3) with the second solution $\varphi = (\hat{p}_1, \hat{q}_1)^t$ of the linear equations (2.1)–(2.2) with $\lambda = \lambda_1$:

$$(5.1) \quad \hat{u} = u + \frac{2(\lambda_1 + \bar{\lambda}_1)\hat{p}_1\bar{\hat{q}}_1}{|\hat{p}_1|^2 + |\hat{q}_1|^2},$$

where u is the periodic standing wave in the form (4.3) and $\varphi = (\hat{p}_1, \hat{q}_1)^T$ is a solution to the linear equations (2.1)–(2.2) for $\lambda = \lambda_1$ written in the form (4.2). Substituting (4.2) into (5.1) yields a more explicit formula:

$$(5.2) \quad \hat{u} = \tilde{u} + \frac{4(\lambda_1 + \bar{\lambda}_1) [(p_1^2\phi_1 - \bar{q}_1^2\bar{\phi}_1)(|p_1|^2 + |q_1|^2) - 4p_1\bar{q}_1]}{(|p_1|^2 + |q_1|^2) [4 + |\phi_1|^2(|p_1|^2 + |q_1|^2)^2]},$$

where $\varphi = (p_1, q_1)^T$ is a periodic solution to the linear equations (2.1)–(2.2) for $\lambda = \lambda_1$ in the form (4.4), ϕ_1 is a linearly growing solution to the system (4.6) and (4.7), and \tilde{u} is given by

$$(5.3) \quad \tilde{u} = u + \frac{2(\lambda_1 + \bar{\lambda}_1)p_1\bar{q}_1}{|p_1|^2 + |q_1|^2}.$$

We will show with explicit analytical computations that \tilde{u} is a translated version of u along symmetries of the NLS equation (1.1). It also follows from (4.10), (4.15), and (4.21) that $|\phi_1(x, t)| \rightarrow \infty$ as $|x| + |t| \rightarrow \infty$ everywhere on the (x, t) -plane with the only exception for the periodic standing wave

with non-trivial phase, parameters of which satisfy the constraint (4.23). Since the representation (5.2) implies that $\hat{u}|_{|\phi_1| \rightarrow \infty} = \tilde{u}$, the aforementioned properties imply that the one-fold transformation (5.1) generates a rogue wave \hat{u} on the background of the periodic standing wave u and the rogue wave satisfies the limits (1.4) with the only exception given by the constraint (4.23).

The representation (5.2) also implies that

$$(5.4) \quad \hat{u}|_{\phi_1=0} = u - \frac{2(\lambda_1 + \bar{\lambda}_1)p_1\bar{q}_1}{|p_1|^2 + |q_1|^2} = 2u - \tilde{u}.$$

We will show numerically that $|\hat{u}|$ has a global maximum at $(x, t) = (0, 0)$, from which we can compute the magnification factor M of the rogue wave \hat{u} according to the definition (1.5). Since $\phi_1(0, 0) = 0$ by the choice of the integration constant in (4.10), (4.15), and (4.21), the magnification factor M is computed from (5.4) as follows:

$$(5.5) \quad M = \frac{|\hat{u}(0, 0)|}{\max_{(x,t) \in \mathbb{R}^2} |\hat{u}|} = \frac{|2u(0, 0) - \tilde{u}(0, 0)|}{\max_{(x,t) \in \mathbb{R}^2} |\tilde{u}(x, t)|} \leq 3,$$

where in the last bound we have used the property that \tilde{u} is a translated version of u . Hence, the magnification factor M of the rogue waves obtained with the one-fold Darboux transformation (5.1) does not exceed the triple magnification factor of the canonical rogue wave (1.2) attained at the constant-amplitude wave background.

5.1. Periodic standing waves with trivial phase. For the dn-periodic wave (3.11), we obtain from (4.3), (4.4), (4.9), and (5.2):

$$(5.6) \quad \hat{u} = \left[\mp \tilde{U} + \frac{2(\phi_1 + \bar{\phi}_1) \frac{dU}{dx} + 4\lambda_1(\phi_1 - \bar{\phi}_1)U + 8(U \pm \tilde{U})}{4 + |\phi_1|^2 U^2} \right] e^{2ibt},$$

where $U(x) = \text{dn}(x; k)$,

$$\tilde{U}(x) = \frac{\sqrt{1 - k^2}}{\text{dn}(x; k)} = U(x + K(k)),$$

as follows from Table 22.4.3 in [28], and $\phi_1(x, t)$ is given by (4.10). Fig. 5 shows rogue waves (5.6) for both signs which correspond to two choices of $\lambda = \frac{1}{2}(u_1 \pm u_2)$ with $u_1 = 1$ and $u_2 = \sqrt{1 - k^2}$.

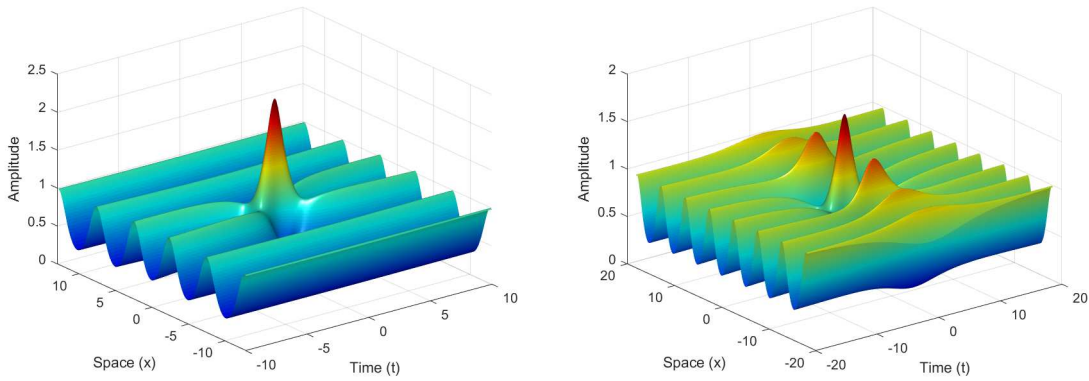


FIGURE 5. Rogue waves on the dn-periodic wave with $k = 0.95$ for eigenvalues $\lambda_1 = \frac{1}{2}(u_1 \pm u_2)$ with upper sign (left) and lower sign (right).

Since $|\phi_1(x, t)| \rightarrow \infty$ as $|x| + |t| \rightarrow \infty$ everywhere on the (x, t) plane, we have $\hat{u}(x, t) \sim \mp \tilde{U}(x) e^{2ibt}$ as $|x| + |t| \rightarrow \infty$, which is a translation of the original periodic standing wave $u(x, t) = U(x) e^{2ibt}$ in

x by a half-period. On the other hand, since $\phi_1(0, 0) = 0$ and the maximum of $|\hat{u}(x, t)|$ occurs at the origin $(x, t) = (0, 0)$ (see Fig. 5), it follows from (5.5) that

$$(5.7) \quad M = \frac{|2U(0) - \tilde{U}(0)|}{\max_{x \in \mathbb{R}} |\tilde{U}(x)|} = 2 \pm \sqrt{1 - k^2},$$

which is the magnification factor of the rogue wave on the dn-periodic wave (3.11) obtained in [15].

For the cn-periodic wave (3.13), we obtain from (4.3), (4.4), (4.9), (4.13), (4.14), and (5.2):

$$(5.8) \quad \hat{u} = \left[\pm i\tilde{U} + \frac{2(\phi_1 + \bar{\phi}_1) \frac{dU}{dx} + 4(\lambda_1 \phi_1 - \bar{\lambda}_1 \bar{\phi}_1)U + 8(U \mp i\tilde{U})}{4 + |\phi_1|^2 \text{dn}^2(x; k)} \right] e^{2ibt},$$

where $U(x) = k \text{cn}(x; k)$,

$$\tilde{U}(x) = -\frac{k\sqrt{1 - k^2} \text{sn}(x; k)}{\text{dn}(x; k)} = U(x + K(k)),$$

as follows from Table 22.4.3 in [28], and $\phi_1(x, t)$ is given by (4.15). Fig. 6 shows rogue wave (5.8) with the upper sign for two choices of k with qualitatively different Lax spectrum on Fig. 2. The two signs in (5.8) correspond to two choices of $\lambda = \frac{1}{2}(u_1 \pm i\nu_2)$ with $u_1 = k$ and $\nu_2 = \sqrt{1 - k^2}$. The rogue wave (5.8) with the lower sign propagates to the opposite direction on the (x, t) plane compared to the rogue wave with the upper sign on Fig. 6.

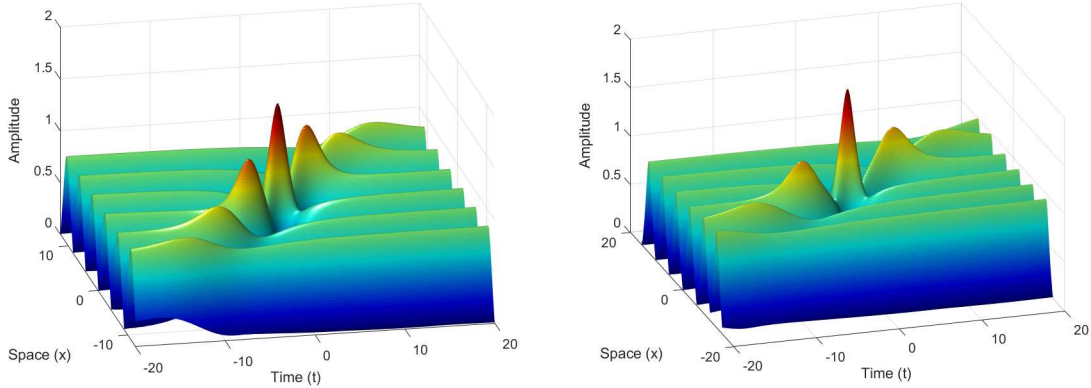


FIGURE 6. Rogue waves on the cn-periodic wave with $k = 0.85$ (left) and $k = 0.95$ (right).

Since $|\phi_1(x, t)| \rightarrow \infty$ as $|x| + |t| \rightarrow \infty$ everywhere on the (x, t) plane, we have $\hat{u}(x, t) \sim \pm i\tilde{U}(x)e^{2ibt}$ as $|x| + |t| \rightarrow \infty$, which is a translation of the original periodic standing wave $u(x, t) = U(x)e^{2ibt}$ in x by a quarter period. On the other hand, since $\phi_1(0, 0) = 0$ and the maximum of $|\hat{u}(x, t)|$ occurs at the origin $(x, t) = (0, 0)$ (see Fig. 6), it follows from (5.5) that

$$(5.9) \quad M = \frac{|2U(0) - \tilde{U}(0)|}{\max_{x \in \mathbb{R}} |\tilde{U}(x)|} = 2,$$

which is the double magnification factor of the rogue wave on the cn-periodic wave (3.13) obtained in [15].

5.2. Periodic standing waves with nontrivial phase. For the periodic standing wave given by $U(x) = R(x)e^{i\Theta(x)}$, we obtain from (4.3), (4.4), (4.18), (4.19), (4.20), and (5.2):

$$(5.10) \quad \hat{u} = \left[\mp \tilde{R} + \frac{4(\sqrt{\rho_1} \pm \sqrt{\rho_2})(\tilde{P}_1^2 \phi_1 - \bar{Q}_1^2 \bar{\phi}_1) + 8(R \pm \tilde{R})}{4 + |\phi_1|^2 \text{dn}^2(x; k)} \right] e^{i\Theta} e^{2ibt},$$

where

$$\tilde{R} = \frac{\sqrt{\rho_1 \rho_2}}{R(x)} - \frac{i\sqrt{-\rho_3}}{\text{dn}^2(x; k)} \frac{dR}{dx}$$

and $\phi_1(x, t)$ is given by (4.21). Fig. 7 shows rogue waves (5.10) for the upper sign (upper panels) and the lower sign (lower panels). The left and right panels correspond to two choices of k with qualitatively different Lax spectrum on Fig. 3. The upper and lower signs correspond to two choices of λ_1 in (4.16).

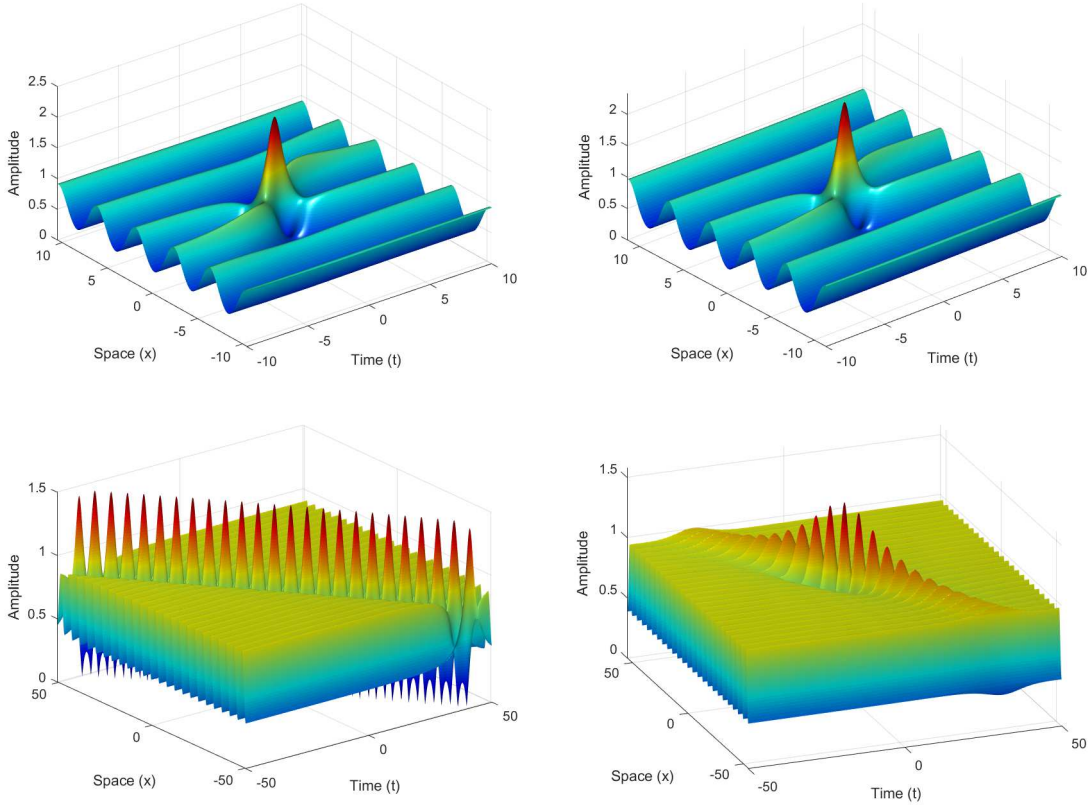


FIGURE 7. Rogue waves on the periodic wave with non-trivial phase for $(\beta, k) = (0.85, 0.85)$ (left) and $(\beta, k) = (0.95, 0.9)$ (right). The upper and lower panels show rogue waves (5.10) with the upper and lower signs respectively.

Since $|\phi_1(x, t)| \rightarrow \infty$ as $|x| + |t| \rightarrow \infty$ everywhere on the (x, t) plane with the only exception for parameters satisfying the constraint (4.23), we have $\hat{u}(x, t) \sim \mp \tilde{R}(x)e^{i\Theta(x)}e^{2ibt}$ as $|x| + |t| \rightarrow \infty$. It

follows from (3.22) that

$$\begin{aligned}
|\tilde{R}(x)|^2 &= \frac{\rho_1 \rho_2}{\rho(x)} - \frac{\rho_3}{4\rho(x) \operatorname{dn}^4(x; k)} \left(\frac{d\rho}{dx} \right)^2 \\
&= \frac{\beta(\beta - k^2) \operatorname{dn}^2(x; k) + (1 - \beta) k^4 \operatorname{sn}^2(x; k) \operatorname{cn}^2(x; k)}{(\beta - k^2 \operatorname{sn}^2(x; k)) \operatorname{dn}^2(x; k)} \\
&= \beta - \frac{k^2 \operatorname{cn}^2(x; k)}{\operatorname{dn}^2(x; k)} \\
&= \beta - k^2 \operatorname{sn}^2(x + K(k); k),
\end{aligned}$$

where the last equality follows from Table 22.4.3 in [28]. Hence $|\tilde{R}(x)|$ is a translation of $R(x)$ in x by a half period. On the other hand, since $\phi_1(0, 0) = 0$, $R(0) = \sqrt{\rho_1}$, and $\frac{dR}{dx}|_{x=0} = 0$, and the maximum of $|\hat{u}(x, t)|$ occurs at the origin $(x, t) = (0, 0)$ (see Fig. 7), it follows from (5.5) that

$$(5.11) \quad M = \frac{|2R(0) \pm \tilde{R}(0)|}{\max_{x \in \mathbb{R}} |\tilde{R}(x)|} = 2 \pm \sqrt{1 - \frac{k^2}{\beta}}.$$

When $\beta = 1$, $M = 2 \pm \sqrt{1 - k^2}$ coincides with the magnification factor (5.7) of the dn -periodic wave (3.11). When $\beta = k^2$, $M = 2$ coincides with the double magnification factor (5.9) of the cn -periodic wave (3.13).

All the solutions on Fig. 7 represent the rogue waves on the background of the periodic standing wave with the exception of the left lower panel, which corresponds to the point $(\beta, k) = (0.85, 0.85)$ near the red curve of Fig. 4 given by the implicit equation (4.23). In this exceptional case, $|\phi_1(x, t)|$ remains bounded along the family of straight lines in the (x, t) plane given by (4.24). As a result, instead of a rogue wave localized on the background of the periodic standing wave, the solution in the exceptional case represents an algebraic soliton propagating on the background of the periodic standing wave. This solution is similar to the algebraic solitons propagating on the modulationally stable dn -periodic waves of the modified KdV equation [14]. Note that the algebraic soliton on the periodic standing wave background does not satisfy the limits (1.4).

6. RELATION TO THE MODULATION INSTABILITY OF THE PERIODIC WAVES

Here we solve the linear equations (2.1)–(2.2) in the case of the periodic standing wave (4.3). The spectral parameter λ is defined in the Lax spectrum of the spectral problem (2.1). Separating variables by

$$(6.1) \quad u(x, t) = U(x)e^{2ibt}, \quad \varphi_1(x, t) = \chi_1(x)e^{ibt+t\Omega}, \quad \varphi_2(x, t) = \chi_2(x)e^{-ibt+t\Omega},$$

where $\Omega \in \mathbb{C}$ is another spectral parameter, yields two spectral problems

$$(6.2) \quad \chi_x = \begin{pmatrix} \lambda & U \\ -\bar{U} & -\lambda \end{pmatrix} \chi, \quad \Omega \chi = i \begin{pmatrix} \lambda^2 + \frac{1}{2}|U|^2 - b & \frac{1}{2}\frac{dU}{dx} + \lambda U \\ \frac{1}{2}\frac{d\bar{U}}{dx} - \lambda \bar{U} & -\lambda^2 - \frac{1}{2}|U|^2 + b \end{pmatrix} \chi.$$

Since the second spectral problem in (6.2) is a linear algebraic system, it admits a nonzero solution if and only if the determinant of the coefficient matrix is zero. The latter condition yields the x -independent relation between Ω and λ in the form $\Omega^2 + P(\lambda) = 0$, where $P(\lambda)$ is given by (2.27) with $c = 0$ and the first-order invariants (2.25) and (2.26) with $c = 0$ have been used.

By Theorem 5.1 in [17], if λ is in the Lax spectrum of the first spectral problem in (6.2), then the squared eigenfunctions χ_1^2 and χ_2^2 determine eigenfunctions of the linearized NLS equation at the periodic standing wave with the eigenvalues given by

$$(6.3) \quad \Gamma = 2\Omega = \pm 2i\sqrt{P(\lambda)}.$$

If $\text{Re}(\Gamma) > 0$ for λ in the Lax spectrum, the periodic standing wave is called *spectrally unstable*. If the instability band intersects the origin in the Γ -plane, the periodic standing wave is called *modulationally unstable*.

The Lax spectrum for λ in the first spectral problem in (6.2) is found with the help of the Floquet–Bloch decomposition in Appendix A. By Theorem 7.1 in [17], $i\mathbb{R}$ belongs to the Lax spectrum and it follows from (3.8) and (3.24) that

$$P(\lambda) > 0 \quad \text{for every } \lambda \in i\mathbb{R},$$

hence $\Gamma \in i\mathbb{R}$ in (6.3) for every $\lambda \in i\mathbb{R}$. Therefore, the spectral instability of the periodic standing wave arises only if λ belongs to the finite band(s) with $\text{Re}(\lambda) \neq 0$, see Figs. 1, 2, and 3. Recently, this conclusion was generalized for other nonlinear integrable equations in [19].

For the dn-periodic wave (3.11) it follows from (3.8) that $P(\lambda) < 0$ for every $|\lambda| \in (\lambda_2^+, \lambda_1^+)$ and $P(\lambda_{1,2}^+) = 0$, where $\lambda_{1,2}^+$ are given by (3.12). The corresponding values of Γ in (6.3) belongs to the finite segment on the real line which touches the origin since $\Gamma = 0$ if $\lambda = \lambda_{1,2}^+$. Hence, the dn-periodic wave (3.11) is modulationally unstable and the rogue waves constructed for $\lambda = \lambda_{1,2}^+$ on Fig. 5 correspond to the end points of the modulation instability band.

Similarly, for the cn-periodic wave (3.13), the trace of Γ in (6.3) on the complex plane is shown on Fig. 8. The curves are obtained when λ changes along the two bands of the Lax spectrum in Fig. 2 with $\text{Re}(\lambda) \neq 0$. Note that each curve on Fig. 8 is covered twice. The modulation instability bands on Fig. 8 are similar for both examples of the cn-periodic wave (3.13) with two different Lax spectrum on Fig. 2. Again, $\Gamma = 0$ at $\lambda = \lambda_{1,2}^+$, hence the rogue waves constructed for $\lambda = \lambda_{1,2}^+$ on Fig. 6 correspond to the end points of the modulation instability band.

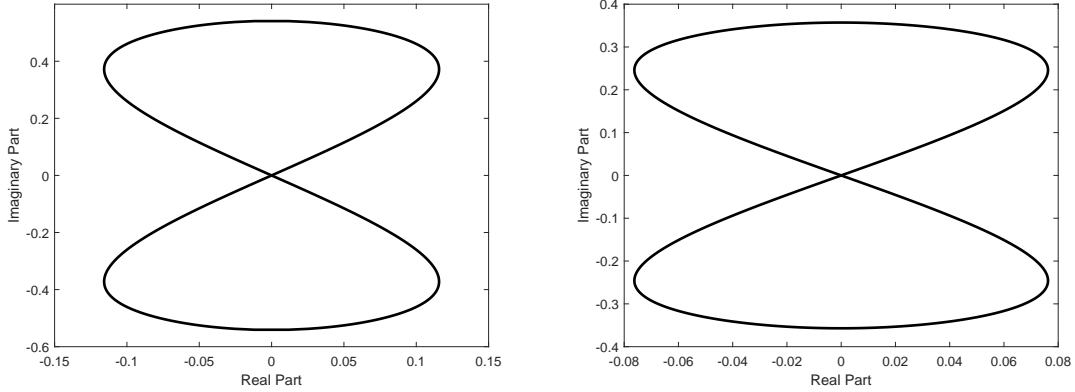


FIGURE 8. Modulation instability bands for the cn-periodic wave (3.13) with $k = 0.85$ (left) and $k = 0.95$ (right).

For the periodic standing wave with non-trivial phase, the trace of Γ in (6.3) is shown on Fig. 9 when λ changes along the two bands of the Lax spectrum on Fig. 3 with $\text{Re}(\lambda) \neq 0$. The symmetry of the Lax spectrum on Fig. 3 is broken and each curve on Fig. 9 is covered once. It follows from Fig. 4 that the point $(\beta, k) = (0.85, 0.85)$ is selected near the boundary (4.23). This boundary coincides with the condition under which the second band of the modulation instability is tangential to the imaginary axis of Γ at $\Gamma = 0$ as on the left panel of Fig. 9. Indeed, the nonlinear equation (4.23) was found in equation (106) in [17] from the above condition.

It follows from different types of the rogue waves in Fig. 7 that the rogue wave on the background of the periodic standing wave satisfying the limits (1.4) exists if the modulation instability band is

transverse to the imaginary axis at $\Gamma = 0$, whereas the algebraic soliton on the periodic standing wave exists if the modulation instability band is tangential to the imaginary axis at $\Gamma = 0$. We emphasize again that the algebraic soliton on the periodic standing wave does not satisfy the limits (1.4).

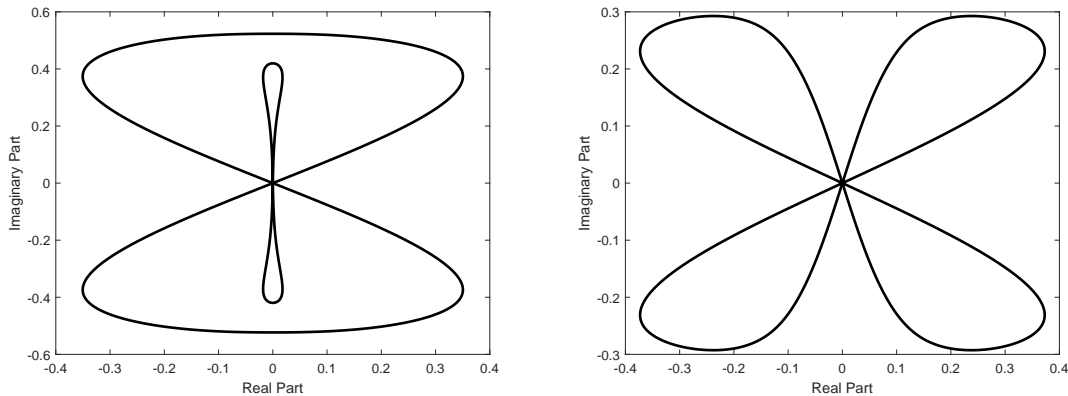


FIGURE 9. Modulation instability bands for the periodic wave (3.22) with $(\beta, k) = (0.85, 0.85)$ (left) and $(\beta, k) = (0.95, 0.9)$ (right).

We conclude the paper by reiterating the question on how to define the parameter λ_1 in the one-fold Darboux transformation (2.3) in order to generate the rogue waves on the background of the periodic standing wave satisfying the limits (1.4). If $\lambda_1 \in i\mathbb{R}$, then $\hat{u} = u$ and no new solution is obtained. If $\lambda_1 \notin i\mathbb{R}$ is outside the other bands of the Lax spectrum, then the one-fold transformation (2.3) generates the recurrent pattern of rogue waves. In the case of the constant-amplitude waves, such recurrent rogue waves are usually referred to as the Kuznetsov–Ma breathers. These rogue waves do not satisfy the limits (1.4).

On the other hand, if $\lambda_1 \notin i\mathbb{R}$ is inside the other bands of the Lax spectrum, then the one-fold transformation (2.3) generates a periodic perturbation on the periodic wave background which grows and decays exponentially in time due to modulation instability with the growth rate Γ in (6.3). In the context of the constant-amplitude wave, the space-periodic and time-localized solutions are usually referred to as the Akhmediev breathers. Since the perturbation period is different from the period of the periodic wave background, such solutions are generally quasi-periodic in space and exponentially localized in time. These rogue waves also satisfy the limits (1.4) but do not represent isolated rogue waves.

Isolated rogue waves on the background of the periodic standing wave are generated by picking the value of λ_1 exactly at the end points of the bands of the Lax spectrum outside $i\mathbb{R}$. Isolated rogue waves satisfy the limits (1.4) with the only exception when $|\phi_1(x, t)|$ remains bounded along a family of the straight lines in the (x, t) -plane, as it happens for the periodic standing wave with parameters satisfying the condition (4.23). This exception which generates an algebraic soliton on the periodic standing wave corresponds to the case when the modulation instability band is tangential to the imaginary axis at $\Gamma = 0$.

The precise values of λ_1 at the end points of the Lax spectrum are captured by the algebraic method with one eigenvalue developed in this article. This method complements the previous characterization of the end points of the bands of the Lax spectrum outside $i\mathbb{R}$ with the resolvent method in [24, 25].

Acknowledgement. Analytical work on this project was supported by the National Natural Science Foundation of China (No. 11971103). Numerical work was supported by the Russian Science Foundation (No.19-12-00253).

APPENDIX A. FLOQUET-BLOCH DECOMPOSITION OF THE LAX SPECTRUM

If the entries of the matrix Q in the linear equation (2.1) are periodic in x with the same period L , then Floquet's Theorem guarantees that bounded solutions of the linear equation (2.1) can be represented in the form:

$$(A.1) \quad \varphi(x) = \begin{pmatrix} \check{p}_1(x) \\ \check{q}_1(x) \end{pmatrix} e^{i\mu x},$$

where $\check{p}_1(x) = \check{p}_1(x + L)$, $\check{q}_1(x) = \check{q}_1(x + L)$, and $\mu \in [-\frac{\pi}{L}, \frac{\pi}{L}]$. The Lax spectrum in the linear equation (2.1) is formed by all admissible values of λ , for which the solutions are bounded in the form (A.1), where $i\mu$ is referred to as the Floquet exponent. When $\mu = 0$ and $\mu = \pm\frac{\pi}{L}$, the solutions (A.1) are periodic and anti-periodic, respectively.

Substituting (A.1) into the linear equation (2.1) and re-arranging the terms yields the eigenvalue problem:

$$(A.2) \quad \begin{pmatrix} \frac{d}{dx} + i\mu & -u \\ -\bar{u} & -\frac{d}{dx} - i\mu \end{pmatrix} \begin{pmatrix} \check{p}_1 \\ \check{q}_1 \end{pmatrix} = \lambda \begin{pmatrix} \check{p}_1 \\ \check{q}_1 \end{pmatrix},$$

for which we are looking for L -periodic solutions $(\check{p}_1, \check{q}_1)$ at a discrete set of admissible values of λ .

The numerical scheme of computing the eigenvalues λ is based on the discretization of the interval $[0, L]$ with $N + 1$ equally spaced grid points and using the highly accurate central difference approximation of derivatives (up to the 12th order of accuracy). MATLAB's eigenvalue solver is used to compute all eigenvalues λ in the discretization of the eigenvalue problem (A.2). Tracing the set of eigenvalues λ for $\mu \in [-\frac{\pi}{L}, \frac{\pi}{L}]$ gives the band of the Lax spectrum in the λ plane shown on Figs. 1, 2, and 3.

APPENDIX B. PROOF OF IDENTITIES (4.19) AND (4.20)

We substitute (4.18) into (4.17), recall that $R^2 \frac{d\Theta}{dx} = -2a = \sqrt{\rho_1 \rho_2} \sqrt{-\rho_3}$, and obtain

$$(B.1) \quad \begin{cases} \tilde{P}_1^2 = \frac{1}{2(\sqrt{\rho_1} \pm \sqrt{\rho_2})} \left(\frac{dR}{dx} + (\sqrt{\rho_1} \pm \sqrt{\rho_2})R + i\sqrt{-\rho_3}(\pm R + \sqrt{\rho_1 \rho_2} R^{-1}) \right), \\ \tilde{Q}_1^2 = \frac{1}{2(\sqrt{\rho_1} \pm \sqrt{\rho_2})} \left(-\frac{dR}{dx} + (\sqrt{\rho_1} \pm \sqrt{\rho_2})R + i\sqrt{-\rho_3}(\pm R + \sqrt{\rho_1 \rho_2} R^{-1}) \right), \\ \tilde{P}_1 \tilde{Q}_1 = -\frac{1}{2(\sqrt{\rho_1} \pm \sqrt{\rho_2})} \left(R^2 \pm \sqrt{\rho_1 \rho_2} \pm i\sqrt{-\rho_3}(\sqrt{\rho_1} \pm \sqrt{\rho_2}) \right). \end{cases}$$

By using (3.16) with (3.19) and $\rho = R^2$, we obtain $(|\tilde{P}_1|^2 + |\tilde{Q}_1|^2)^2 = \rho(x) - \rho_3 = \text{dn}^2(x; k)$, where the last identity follows from (3.22). Extracting the square root yields (4.19).

In order to prove (4.20), we compute from (B.1):

$$\tilde{P}_1^2 \tilde{Q}_1^2 = \frac{\left[-\left(\frac{dR}{dx} \right)^2 + (\sqrt{\rho_1} \pm \sqrt{\rho_2})^2 R^2 - \rho_3 (\pm R^2 + \sqrt{\rho_1 \rho_2} R^{-1})^2 - 2i\sqrt{-\rho_3}(\pm R^2 + \sqrt{\rho_1 \rho_2} R^{-1}) \frac{dR}{dx} \right]}{4(\sqrt{\rho_1} \pm \sqrt{\rho_2})^2}.$$

By using (3.16) with (3.19) and (3.22), we check directly that

$$-\left(\frac{dR}{dx} \right)^2 + (\sqrt{\rho_1} \pm \sqrt{\rho_2})^2 R^2 - \rho_3 (\pm R^2 + \sqrt{\rho_1 \rho_2} R^{-1})^2 = \frac{\text{dn}^2(x; k)}{R^2} (\pm R^2 + \sqrt{\rho_1 \rho_2})^2 + \frac{\rho_3}{\text{dn}^2(x; k)} \left(\frac{dR}{dx} \right)^2,$$

which yields

$$\tilde{P}_1^2 \tilde{Q}_1^2 = \frac{1}{4(\sqrt{\rho_1} \pm \sqrt{\rho_2})^2} \left[\frac{\text{dn}(x; k)}{R} (\pm R^2 + \sqrt{\rho_1 \rho_2}) - \frac{i\sqrt{-\rho_3}}{\text{dn}(x; k)} \frac{dR}{dx} \right]^2.$$

Extracting the square root and picking the negative sign by using the limiting expression (4.14) for $\rho_1 = k^2$, $\rho_2 = 0$, and $\rho_3 = -(1 - k^2)$ yields the expression (4.20).

REFERENCES

- [1] D.S. Agafontsev and V.E. Zakharov, “Integrable turbulence and formation of rogue waves”, *Nonlinearity* **28** (2015), 2791–2821.
- [2] D.S. Agafontsev and V.E. Zakharov, “Integrable turbulence generated from modulational instability of cnoidal waves”, *Nonlinearity* **29** (2016), 3551–3578.
- [3] N.N. Akhmediev, V.M. Eleonsky, and N.E. Kulagin, “Generation of periodic trains of picosecond pulses in an optical fiber: Exact solutions”, *Sov. Phys. JETP* **62** (1985), 894–899.
- [4] N. Akhmediev, A. Ankiewicz, and J.M. Soto-Crespo, “Rogue waves and rational solutions of the nonlinear Schrödinger equation”, *Phys. Rev. E* **80** (2009), 026601 (9 pages).
- [5] M. Bertola, G.A. El, and A. Tovbis, “Rogue waves in multiphase solutions of the focusing nonlinear Schrödinger equation”, *Proc. R. Soc. Lond. A* **472** (2016), 20160340 (12 pages).
- [6] M. Bertola and A. Tovbis, “Maximal amplitudes of finite-gap solutions for the focusing nonlinear Schrödinger equation”, *Comm. Math. Phys.* **354** (2017), 525–547.
- [7] D. Bilman and R. Buckingham, “Large-order asymptotics for multiple-pole solitons of the focusing nonlinear Schrödinger equation”, *J. Nonlinear Sci.* **29** (2019), 2185–2229.
- [8] D. Bilman and P. D. Miller, “A robust inverse scattering transform for the focusing nonlinear Schrödinger equation”, *Comm. Pure Appl. Math.* **72** (2019), 1722–1805.
- [9] D. Bilman, L. Ling and P.D. Miller, “Extreme superposition: rogue waves of infinite order and the Painlevé-III hierarchy”, arXiv:1806.00545 (2018).
- [10] G. Biondini, S. Li, D. Mantzavinos, and S. Trillo, “Universal behavior of modulationally unstable media”, *SIAM Review* **60** (2018), 888–908.
- [11] J.C. Bronski, V.M. Hur, and M.A. Johnson, “Modulational instability in equations of KdV type”, in *New approaches to nonlinear waves*, Lecture Notes in Phys. **908** (Springer, Cham, 2016), pp. 83–133.
- [12] A. Calini and C.M. Schober, “Characterizing JONSWAP rogue waves and their statistics via inverse spectral data”, *Wave Motion* **71** (2017), 5–17.
- [13] C.W. Cao and X.G. Geng, “Classical integrable systems generated through nonlinearization of eigenvalue problems”, *Nonlinear physics (Shanghai, 1989)*, pp. 68–78 (Research Reports in Physics, Springer, Berlin, 1990).
- [14] J. Chen and D.E. Pelinovsky, “Rogue periodic waves in the modified Korteweg-de Vries equation”, *Nonlinearity* **31** (2018), 1955–1980.
- [15] J. Chen and D.E. Pelinovsky, “Rogue periodic waves in the focusing nonlinear Schrödinger equation”, *Proc. R. Soc. Lond. A* **474** (2018), 20170814 (18 pages).
- [16] J. Chen, D.E. Pelinovsky, and R.E. White, “Rogue waves on the double-periodic background in the focusing nonlinear Schrödinger equation”, *Phys. Rev. E* **100** (2019), 052219 (18 pages).
- [17] B. Deconinck and B.L. Segal, “The stability spectrum for elliptic solutions to the focusing NLS equation”, *Physica D* **346** (2017), 1–19.
- [18] B. Deconinck and J. Upsal, “The orbital stability of elliptic solutions of the focusing nonlinear Schrödinger equation”, arXiv: 1901.08702 (2019).
- [19] B. Deconinck and J. Upsal, “Real Lax spectrum implies spectral stability”, arXiv: 1909.10119 (2019).
- [20] P. Dubard and V.B. Matveev, “Multi-rogue waves solutions: from the NLS to the KP-I equation”, *Nonlinearity* **26** (2013), R93–R125.
- [21] B.F. Feng, L. Ling, and D.A. Takahashi, “Multi-breathers and high order rogue waves for the nonlinear Schrödinger equation on the elliptic function background”, *Stud. Appl. Math.* (2020), in press.
- [22] P.G. Grinevich and P.M. Santini, “The finite gap method and the analytic description of the exact rogue wave recurrence in the periodic NLS Cauchy problem”, *Nonlinearity* **31** (2018), 5258–5308.
- [23] P.G. Grinevich and P.M. Santini, “The finite gap method and the periodic NLS Cauchy problem of the anomalous waves, for a finite number of unstable modes”, *Russ. Math. Surv.* **74** (2019), 211–263.
- [24] A.M. Kamchatnov, “On improving the effectiveness of periodic solutions of the NLS and DNLS equations”, *J. Phys. A: Math. Gen.* **23** (1990), 2945–2960.
- [25] A.M. Kamchatnov, “New approach to periodic solutions of integrable equations and nonlinear theory of modulational instability”, *Phys. Rep.* **286** (1997), 199–270.
- [26] D.J. Kedziora, A. Ankiewicz, and N. Akhmediev, “Rogue waves and solitons on a cnoidal background”, *Eur. Phys. J. Special Topics* **223** (2014), 43–62.

- [27] Y. Ohta and J. Yang, “General high-order rogue waves and their dynamics in the nonlinear Schrödinger equation”, *Proc. R. Soc. Lond. A* **468** (2012), 1716–1740.
- [28] F.W.J. Olver, D.W. Lozier, R.F. Boisvert, and C.W. Clark, “NIST Handbook of Mathematical Functions”, Cambridge University Press, ISBN: 978-0-521-19225-5, (2010).
- [29] D.H. Peregrine, “Water waves, nonlinear Schrödinger equations and their solutions”, *J. Austral. Math. Soc. B.* **25** (1983), 16–43.
- [30] V.E. Zakharov and L.A. Ostrovsky, “Modulation instability: The beginning”, *Physica D* **238** (2009), 540–548.
- [31] R.G. Zhou, “Nonlinearization of spectral problems of the nonlinear Schrödinger equation and the real-valued modified Korteweg de Vries equation”, *J. Math. Phys.* **48** (2007), 013510 (9 pages).
- [32] R.G. Zhou, “Finite-dimensional integrable Hamiltonian systems related to the nonlinear Schrödinger equation”, *Stud. Appl. Math.* **123** (2009), 311–335.

(J. Chen) SCHOOL OF MATHEMATICS, SOUTHEAST UNIVERSITY, NANJING, JIANGSU 210096, P.R. CHINA
E-mail address: `cjb@seu.edu.cn`

(D.E. Pelinovsky) DEPARTMENT OF MATHEMATICS, MCMASTER UNIVERSITY, HAMILTON, ONTARIO, CANADA, L8S 4K1
E-mail address: `dmpeli@math.mcmaster.ca`

(D.E. Pelinovsky) INSTITUTE OF APPLIED PHYSICS RAS, NIZHNY NOVGOROD, 603950, RUSSIA

(R.E. White) DEPARTMENT OF MATHEMATICS, MCMASTER UNIVERSITY, HAMILTON, ONTARIO, CANADA, L8S 4K1
E-mail address: `whitere@mcmaster.ca`